



Reduction Pilot Contamination in Downlink Multi-Cell for Massive MIMO Systems

Adeeb Salh¹, Lukman Audah^{1*}, Nor Shahida Mohd Shah¹, Shipun Anuar Hamzah¹

¹Wireless and Radio Science Center (WARAS)
Faculty of Electrical and Electronic Engineering, Universiti Tun Hussein Onn Malaysia
86400 Parit Raja, Batu Pahat, Johor, MALAYSIA

*Corresponding author

DOI: <https://doi.org/10.30880/ijie.2019.11.08.013>

Received 7 June 2018; Accepted 21 July 2019; Available online 30 December 2019

Abstract: Massive multiple-input-multiple-output has become an important fifth-generation (5G) wireless communication system because it improves transmitted spectral efficiency. In this paper, we obtained the maximal spectral efficiency by improving transmission performance in cell edges. This was achieved by using pilot reuse sequences from all available pilots in order to mitigate the pilot contamination and to suppress interference between adjacent cells. In addition, we investigated the impacts of pilot contamination on the received signal-to-interference-noise ratios (SINR) of users and employed different pilot reuse. We propose a new method called cell-edge-aware maximum ratio transmission (MRT), zero forcing (ZF), and return zero forcing (R-ZF). These were the precoders that employed less spatial dimensions and were able to suppress adjacent cells interference of the maximally vulnerable active user. We conclude that the large pilot reuse value between neighboring cells increased the gain, avoided interference between adjacent cells, and gave the maximal spectral efficiency. Consequently, the R-ZF was better than ZF and MRT because it was able to suppress the SINR.

Keywords: Massive MIMO, spectral efficiency (SE), signal-to-interference-noise ratios, fifth-generation

1. Introduction

Massive multiple-input-multiple-output (MIMO) is very important in fifth-generation (5G) technology, because it allows the achievement of a high data rate, strong interference suppression, and increased multiplicity [1]. A major challenge in mobile broadband networks is how to support the throughput in the future 5G. A massive MIMO system, which exploits a huge number of antennas array at the base station (BS) is able to assist ten users equipment and this technique may suffer from pilot contamination due to inter-cell interference which cannot be fully eliminated. In the multi-cell systems, it is impossible to assign orthogonal pilot sequences for all users in all cells, due to the limitation of the channel coherence interval [2]. In this way, it determines the key to increase spectral efficiency (SE) in modern techniques [3], to provide high data rates for active users (UEs), including those located at the cell edge, without sacrificing the quality of service (QoS) [4].

The estimation channel are used in both of the uplink and downlink by exploiting the channel reciprocity in time division duplex (TDD), where pilot contamination occurs when the pilot reuse sequences are transmitted from all users at the same cell and at the same time to all adjacent cells. The spatial dimensions available at the BS and large diversity of gain can suppress the interference that active cell edge users experienced. Meanwhile, large numbers of cell edge users suffer from pilot contamination when the edge area is small. Consequently, the challenges appear due to interference, at

the edges between the neighboring cells, affecting the signals transmitted to many users in different cells. According to [5], the capacity in the cell-edge could be enhanced by assigning non-overlapping pilot sub bands. Mitigation of inter-cell interference in TDD mode required all users to send pilot signals, which were orthogonal to other users inside these cells as explained in [6]. In other words, UEs at the edge of the cell suffered from strict pilot contamination, which resulted in poor QoS. The channel state information (CSI) obtained the channel's status by transmitting predefined pilot sequences to evaluate the response of the channel [7]. From the previous method in [8], the authors used coalition game theory to achieve high SE. The proposed coalition game theory applied pilot reused method to serve many users because every cell had limited number of pilots by channel coherence. The worst case of pilot contamination occurred when all UEs reused the same pilot sequence to all neighbouring cells at the same time [9]. In this paper, we focus on how to obtain the maximal SE by improving the transmission performance in cell edges: We investigated the effects of pilot contamination on the received SINRs of UEs by employing different pilot reuse sequence. The pilot contamination for multiple cells could be avoided by using the mutually orthogonal pilot sequence.

2. System Model

The multi-cell massive MIMO system consisted of L cells. Each BS was equipped with an array of many antennas M and UEs K had a single antenna, where $M \gg K$. The pilot signal was transmitted by UEs k th in cell l . Determining the status of the CSI required the comparison of the received pilot from every UE with the recognized pilot signal associated with that UE, where the pilot reuse sequence is given by $\beta_{jlk} = \text{diag}\{\beta_{jl1}, \beta_{jl2}, \dots, \beta_{jlk}\}$. In addition, the channel vector between the BS and UEs is given by $h_{jlk} = \sqrt{\beta_{jl}}H_{jl}$. We assumed that the channel reciprocities were the same in both uplink and downlink. The received signal $y_j \in C^M$ at BS j in the downlink is:

$$y_j = \sqrt{Q_d} \sum_{l=1}^L h_{jlk} \gamma_{lk} \mathcal{X}_{lk} + n_{jk} \tag{1}$$

where $H_{jl} = [h_{jl1}, h_{jl2}, \dots, h_{jlK}]^T \in C^{K \times M}$ is the downlink channel matrix, $\sqrt{Q_d}$ is the equal power that UEs K transmitted simultaneously; $n_j \sim CN(0, I_K)$ is a vector of white, zero-mean Gaussian noise, and $\mathcal{X}_{lk} \in C^M$ represents the information vector. Then the received signal in terms of the pilot matrix is given by:

$$Y_\beta = \sqrt{\beta_{jl} Q_d} h_{jlk} \gamma_{lk} + \eta_\beta \tag{2}$$

where γ_{lk} is the precoding matrix from the BS to UEs.

2.1 Pilot Based Channel Estimation

The channel estimation used the training phase to reduce the interference on the pilot sequences. Pilot contamination occurred when all users reused the same pilot to all adjacent cells. Limited channel coherence interval required finite number of pilot reuse sequences. Based on the orthogonality property of MMSE channel estimation during the training phase and uncorrelated channel, the interference on the pilot sequences could be reduced, where the estimation error is:

$$\hat{h}_{jlk}^H = h_{jlk} - \tilde{h}_{jlk}^H \tag{3}$$

Suppressing the interference between adjacent cells and obtaining the conventional pilot reuse were based on the relative channel estimation. The received signal from BS j to active users (UEs) k in cell l can be estimated as follows:

$$\tilde{h}_{jlk} = \frac{\sqrt{Q_t}}{\phi_{jk}} \tilde{h}_{jlk}^H \tag{4}$$

Channel estimation depended on pilot signals i_{lk} , and precoding vector ϕ_{jk} which allowed users to employ the same pilot in the same direction. Due to short coherence interval the orthogonal pilot reuse sequences needed symbols $K \times M$ to mitigate pilot contamination in multi-cell massive MIMO system. The CSI could obtain the channel's status by transmitting predefined pilot sequences to evaluate the response of the channel. The estimation of the covariance matrix can be expressed as $C_{jlk} = \mathbb{E}(\tilde{h}_{jlk}^H, \tilde{h}_{jlk})$. The evaluation of a channel by the covariance matrix is expressed as

$$\mathbb{E} \left[|\tilde{h}_{jlk}^H \phi_{jlk}|^2 \right] = M \left(\text{tr} \left(C_{\hat{h}_{jlk}^H \hat{h}_{jlk}} \right) + K \text{tr} \left(C_{\tilde{h}_{jlk}^H, \tilde{h}_{jlk}} \right) \right) \tag{5}$$

From (5), the SE is achieved by treating the interference, $\tilde{h}_{jlk}^H \phi_{jlk}$ as noise for an arbitrary Gaussian interference, and also treating the uncorrelated interference. The orthogonal pilot sequences in the case of pilot reuse, the vector signal from UEs in cell l is $\mathcal{X}_{lk} = \hat{u}_{ijk}^H \hat{u}_{ilm} = B$, where $1 \leq B \leq S$ and $B \cong K(\beta_{jl} + (1 - \beta_{jl}) \beta_{jl})$. The pilot sequence in the cell centre and cell edge can be determined as follows:

$$\sum_{l \in L} \sum_{m=1}^K F_{jl}^\Omega \hat{u}_{ijk} \hat{u}_{ijk}^H = \sum_{l \in L} \sum_{m=\ell_l}^K F_{j,\ell_l}^\Omega \hat{u}_{ilm} \hat{u}_{ijk}^H + \sum_{l \in L} \sum_{m=\varepsilon_j}^K F_{j,\varepsilon_j}^\Omega \hat{u}_{ilm} \hat{u}_{ijk}^H \quad (6)$$

$$= B \left(\beta_{jl} K \sum_{l \in L} F_{j,\ell_l}^\Omega + (1 - \beta_{jl} K) \sum_{l=\varepsilon_j}^K F_{j,\varepsilon_j}^\Omega \right) \quad (7)$$

where $\Omega = 1, 2$ and F_{jl}^Ω , the propagation parameters, are equal to 1 for $j = 1$ and 2 for $j \neq 1$. The ratio $F_{jl}^\Omega = \vartheta_{jlm}/\vartheta_{llm}$ expresses the relative strength of the interference experienced at the BS j due to user K in the cell l . The covariance matrix channel is given by

$$C_{\tilde{h}_{jlk}^H, \tilde{h}_{jlk}} = \left(\sum_{i \neq l} Q_t \beta_{jlk} K^2 + \sum_{i \neq l} Q_t K + K \right) I_M Q_t K \beta_{jlk} I_M \quad (8)$$

$$\tilde{h}_{jlk}^H = \sum_{i \in l} \sqrt{Q_t \beta_{jlk}} K h_{ijk} + \sum_{i \neq l} \sum_{k=1}^K \sqrt{Q_t \beta_k} \phi_{ijk} \gamma_{ilk} + n_j \quad (9)$$

The precoding vectors from BS in cell j , for UEs k th in cell l becomes

$$\phi_{jlk} = \sum_{i \in l} Q_t \beta_{jk} K + \sum_{i \neq l} \sum_{k=1}^K \frac{Q_t}{K} \left(1 + \frac{Q_t}{K} \left(Q_t \left(1 - \frac{1}{M} \right) \right) \right) \quad (10)$$

Pilot contamination was mitigated by determining the location of users $\vartheta_{jlk} = [\vartheta_{j1l} \dots \vartheta_{jKl}]^T \sim CN(0, I_K)$ inside the cells. The vector signal from UEs in cell l was normally the pilot reuse sequences $\beta_{jl} > 1$; however, a lesser fraction of the cell used similar pilot symbols. The vector signal in cells' channel estimation is given as:

$$\tilde{h}_{jlk} = \sqrt{Q_{lk}} d_j(\vartheta_{lk}) \hat{H}_v \mathcal{E}_{ilk} \quad (11)$$

where, \mathcal{E}_{ilk} denotes the i th column of the identity matrix I_B . According to (11) the MMSE channel estimation depended only on users K which used the same pilot reuse in cell l . To determine the number of pilot reuse sequence in both the cell center and the cell edge, where $\beta_{jl} = \ell_{\ell_l}/K$ or $\beta_{jl} = \varepsilon_j/K$, $I_{\ell_l(k)}$ is defined as:

$$I_{\ell_l(k)} = \begin{cases} 1 & \text{if } K \in \ell_{\ell_l} & \text{center cells} \\ 0 & \text{if } K \in \varepsilon_j & \text{edge cells} \end{cases} \quad (12)$$

where ℓ_{ℓ_l} , ε_j represents the number of users in both of cell center and cell edges respectively.

2.2 Achievable SE for DL Transmission

The achievable SE for users were uniformly distributed within the cell j , and the total SE in cell j is given by:

$$SE_{jK} = \sum_{k=1}^K \left(\left(1 - \frac{B}{S} \right) \log_2(1 + \Gamma_{jk}) \right) \quad (13)$$

The relative strength of the interference received signal at BS j from user K in cell l depended on the propagation environment and the number of the schedule users of channel covariance matrix $C_{\tilde{h}_{jlk}^H, \tilde{h}_{jlk}}$ with orthogonal pilot. To simplify (14) and ease its derivation. The signal to-noise ratio (SNR) is defined as:

$$\Gamma_{jk}^{dl} = \frac{\hat{u}_{ijk}^H C_{\tilde{h}_{jlk}^H, \tilde{h}_{jlk}} \hat{u}_{ijk}}{\sum_{j \in L} \sum_{m=1}^K \left(\frac{d_j(\vartheta_{lm})}{d_l(\vartheta_{lm})} \right) \frac{1}{M} + \left(\frac{d_j(\vartheta_{lm})}{d_l(\vartheta_{lm})} \right)^2 \hat{u}_{ijk}^H \hat{u}_{ijk} C_{\tilde{h}_{jlk}^H, \tilde{h}_{jlk}} - \hat{u}_{ijk}^H C_{\tilde{h}_{jlk}^H, \tilde{h}_{jlk}} \hat{u}_{ijk} + \frac{\sigma^2}{M\rho}} \quad (14)$$

where \hat{u}_{ijk}^H is the linear receive combining vector, σ^{dl}/ρ represents covariance matrix for SINR and $\vartheta_{jlm}/\vartheta_{llm}$ is the location of users.

In reducing the effect of interference between neighboring cells due to the movement of UEs, one should update the CSI and training channel coherence linearly from BS M to all UEs K . Where, employing orthogonal pilot subsets in adjacent cells, optimizing the number of required subsets and the number of scheduled users per cell that maximizes the overall SE for both uplink and downlink [10], [11], [12] and [13]. The cell-edge aware used spatial dimensions to mitigate interference between adjacent cells. The three linear precoders MRT, ZF, and R-ZF, are:

$$A = \begin{cases} \hat{h}_{jjk} & MRT \\ \hat{H}_{vj}E_j(E_j^H\hat{H}_{vj}^H\hat{H}_{vj}E_j)^{-1} & ZF \\ \hat{H}_{vj}(\hat{H}_{vj}^H\hat{H}_{vj} + Z_j^{dl} + M\varphi_j^{dl}I_B)^{-1} & R - ZF \end{cases} \quad (15)$$

where, ρ_{dl} is the effective training SNR, $\varphi_j^{dl} = 1/M\rho_{dl}$ represents the design parameter and $Z_j = \mathbb{E}(\hat{H}_j\hat{H}_j^H + \sum_{l \neq j} \hat{H}_j\hat{H}_j^H)$ is the inter-cell interference matrix for channel estimation. The interference $\Gamma_{l \in \ell_l}^{mrt}$ depended on the linear precoding MRT. We derived the expectations in terms of Γ_{jk}^{dl} based on (12), where the $\Gamma_{l \in \ell_l}^{mrt}$ in the cell centre with respect to the channel realization for MRT can be obtained as follows:

$$\Gamma_{l \in \ell_l}^{mrt} = \frac{[F_{j,\ell_l}^{(2)} - (F_{j,\ell_l}^{(1)})^2]^B}{B \sum_{l \in l_j \setminus \{j\}} \left(F_{j,\ell_l}^2 + \frac{F_{j,\ell_l}^2 - (F_{j,\ell_l}^2)^2}{M} \right) + \left(\sum_{l \in l_j \setminus \{j\}} F_{j,\ell_l}^1 \frac{K}{M} + \frac{\sigma^2}{M\rho} \right) \left(B \sum_{l \in l_j \setminus \{j\}} F_{j,\ell_l}^1 + \frac{\sigma^2}{\rho} \right)} \quad (16)$$

To reduce the interference at the cell edge, the positions of the users were moved according to the denominator (17). We used the reuse pilot sequence at cell edge $\beta_{jl} = \varepsilon_j/K$, $l \in l_j$ the MRT was independent in the other users in the same cell, which is written as follows:

$$\Gamma_{l \in \varepsilon_j}^{mrt} \triangleq \frac{[F_{j,\varepsilon_j}^{(2)} - (F_{j,\varepsilon_j}^{(1)})^2]^{M-B}}{B \sum_{l \in l_j \setminus \{j\}} \left(F_{j,\varepsilon_j}^2 + \frac{F_{j,\varepsilon_j}^2 - (F_{j,\varepsilon_j}^2)^2}{M} \right) + \left(\sum_{l \in \varepsilon_j \setminus \{j\}} F_{j,\varepsilon_j}^1 \frac{K}{M} + \frac{\sigma^2}{M\rho} \right) \left(B \sum_{l \in \varepsilon_j \setminus \{j\}} F_{j,\varepsilon_j}^1 + \frac{\sigma^2}{\rho} \right)} \quad (17)$$

If all users inside the cell had the same distributed F_{j,ε_j}^Q , in this case the distributed loses F_{j,ε_j}^Q depended on K . Moreover, when all available pilot reuse β had been estimated and $\beta > K$ the BS j was able to suppress parts of the interference between the neighboring cells. In multi-cell, the ZF precoding exploits and orthogonalizes all available directions in order to mitigate the inter-cell interference [13], [14], and [15]. The SINR ($\Gamma_{l \in \ell_l}^{zf}$) at the cell centres, is given as:

$$\Gamma_{l \in \ell_l}^{zf} \triangleq \frac{[F_{j,\ell_l}^{(2)} - (F_{j,\ell_l}^{(1)})^2]^B}{B \sum_{l \in l_j \setminus \{j\}} \left(F_{j,\ell_l}^{(2)} + \frac{F_{j,\ell_l}^{(2)} - (F_{j,\ell_l}^{(1)})^2}{M-K} \right) + \frac{\beta_{jl}KM}{\sqrt{M-K}} \left(\sum_{l \in l_j} F_{j,\ell_l}^{(1)} \left(1 - \frac{F_{j,\ell_l}^{(1)}}{\sum_{l \in L_j} F_{j,\ell_l}^{(1)} + \frac{\sigma^2}{B\rho}} \right) \right) \left(B \sum_{l \in L_j} F_{j,\ell_l}^{(1)} + \frac{\sigma^2}{\rho} \right)} \quad (18)$$

To reduce the interference due to multi-user signals, we used ZF to cancel the interference by scheduled UEs per cell completely, using the SINR ($\Gamma_{l \in \ell_l}^{zf}$) at cell edges, when $\beta_{jl} = \varepsilon_j/K$, given by:

$$\Gamma_{l \in \varepsilon_j}^{zf} \triangleq \frac{[F_{j,\varepsilon_j}^{(2)} - (F_{j,\varepsilon_j}^{(1)})^2]^{M-B}}{B \sum_{l \in l_j \setminus \{j\}} \left(F_{j,\varepsilon_j}^{(2)} + \frac{F_{j,\varepsilon_j}^{(2)} - (F_{j,\varepsilon_j}^{(1)})^2}{M-K} \right) + \frac{(1-\beta_{jl})KM}{\sqrt{M-K}} \left(\sum_{l \in \varepsilon_j} F_{j,\varepsilon_j}^{(1)} \left(1 - \frac{F_{j,\varepsilon_j}^{(1)}}{\sum_{l \in \varepsilon_j} F_{j,\varepsilon_j}^{(1)} + \frac{\sigma^2}{B\rho}} \right) \right) \left(B \sum_{l \in \varepsilon_j} F_{j,\varepsilon_j}^{(1)} + \frac{\sigma^2}{\rho} \right)} \quad (19)$$

Cancelling the multiuser interference for every user at the cell edge required the use of linear precoding R-ZF, which exploited all orthogonalized estimated channels at BS. The SINR ($\Gamma_{l \in l \setminus \{j\}}^{R-zf}$) at the cell centres are given by:

$$\Gamma_{l \in \ell_l}^{R-zf} \triangleq \frac{[F_{j,\ell_l}^{(2)} - (F_{j,\ell_l}^{(1)})^2]^B}{B \sum_{l \in l_j \setminus \{j\}} \left(F_{j,\ell_l}^{(2)} + \frac{F_{j,\ell_l}^{(2)} - (F_{j,\ell_l}^{(1)})^2}{M-B} \right) + \frac{(\beta_{jl})KM}{\sqrt{M-K}} \left(\sum_{l \in l_j} F_{j,\ell_l}^{(1)} \left(1 - \frac{F_{j,\ell_l}^{(1)}}{\sum_{l \in L_j} F_{j,\ell_l}^{(1)} + \frac{\sigma^2}{B\rho}} \right) \right) \left(B \sum_{l \in L_j} F_{j,\ell_l}^{(1)} + \frac{\sigma^2}{\rho} \right)} \quad (20)$$

According to the derivation in (19), the respective channel realization in terms of R-ZF, in the denominator ($M - B$), we used (21) to obtain the number of pilot reuse sequences at the cell edges when $\beta_{jl} = \varepsilon_j/K$

$$\Gamma_{l \in \mathcal{E}_j}^{R-ZF} \triangleq \frac{\left[F_{j,\epsilon_j}^{(2)} - \left(F_{j,\epsilon_j}^{(1)} \right)^2 \right]^{M-B}}{B \sum_{l \in \mathcal{E}_j \setminus \{j\}} \left(F_{j,\epsilon_j}^{(2)} + \frac{F_{j,\epsilon_j}^{(2)} - \left(F_{j,\epsilon_j}^{(1)} \right)^2}{M-B} \right) + \frac{(1-\beta_{jl})KM}{\sqrt{M-B}} \left(\sum_{l \in \mathcal{E}_j} F_{j,\epsilon_j}^{(1)} \left(1 - \frac{F_{j,\epsilon_j}^{(1)}}{\sum_{l \in \mathcal{E}_j} F_{j,\epsilon_j}^{(1)} + \frac{\sigma^2}{\rho}} \right) \right) (B \sum_{l \in \mathcal{E}_j} F_{j,\epsilon_j}^{(1)} + \frac{\sigma^2}{\rho})} \quad (21)$$

The first term in each of (16), (17), (18), (19), (20), and (21), describes that the interference (same pilot reuse) was caused by pilot contamination. The second term was caused by the other users with orthogonal pilot sequences, which required used correlated received pilot reuse and channel estimation. The pilot signal at BS, the average received power, depended on the transmitted power and path loss of the edge UEs to obtain the better Γ^{R-ZF} from non-orthogonal pilot transmissions in the neighboring cells [16, 17].

Minimizing SINR saturation due to inter-user interference and the reuse of the same pilot in different cells required the number of UEs to be proportional to the pilot symbols when $M \rightarrow \infty$ for all MRT, ZF and R-ZF. The closed form equation to achieve SE in cell j was derived according to (22), if the subset of cells used the same pilots as the cell in the downlink. The maximized SE was achieved when the $M \rightarrow \infty$ for all cells were based on the distributed number of users according to the pre-log factor in (22) when $K = (S/\beta_{jl})$. Therefore, the maximum numbers of pilot reuse sequences that could be accomplished depended on channel coherence interval S . From all the equations above, we added the difference (relative strength) of the interference received at the BS for cells with the same pilots, as in the origin, but different reuse sequences. Therefore, these techniques had a very encouraging sum of SE gains over conventional multi-cell ZF for a large number of orthogonal pilot reuses and numbers of users. We obtained the maximum SE by combining schemes such as ZF, MRT, and R-ZF as follows:

$$SE_j^{MRT,ZF,R-ZF} = \sum_{k=1}^K \left(1 - \frac{\beta_{jl}K}{S} \right) \log_2 \left(1 + \Gamma^{MRT,ZF,R-ZF}_{jk} \right) \quad (22)$$

where $\left(1 - \frac{\beta_{jl}K}{S} \right)$ represents the loss of pilot signaling for the pre-log factor, and S represents the coherence block interval.

3. Numerical Results

From Fig. 1, it is noted that, with the increase in the number of antenna arrays at the BS, the achievable SE increase per cell depended on the employment of different pilot reuse sequences. Consequently, the large pilot reuse value between neighboring cells $\beta = 7$ increased the gain, avoided the interference between adjacent cells, and gave a high SE performance because this pilot returned different frequency reuse to many neighboring cells in the same cluster. The high achievable SE was dependent on the increasing value of $\beta = \{7, 4, 3, 1\}$. Furthermore, when employing the same pilot reuse between neighboring cells, the pilot contamination increased. This is because pilot reuse utilized the same pilot between adjacent cells and it could not avoid the interference between adjacent cells in the same cluster accurately. Employing more pilot reuse sequences decreased the pilot contamination at the cost of time-consuming training period.

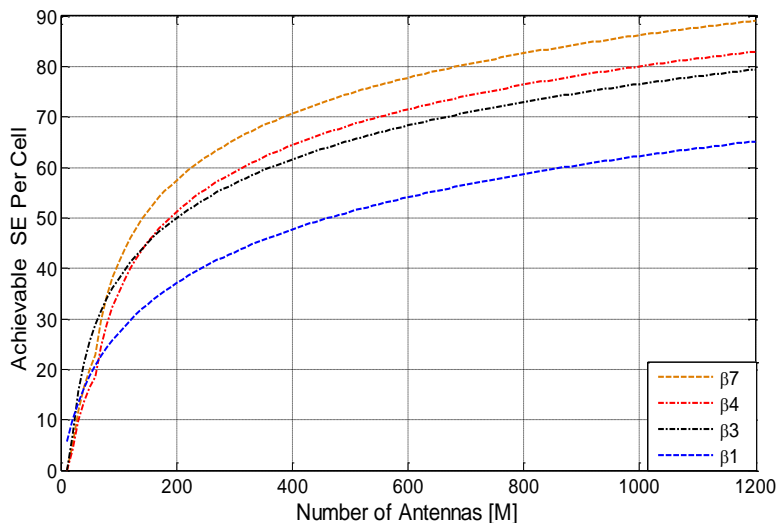


Fig. 1 Achievable SE with number of antennas M , for $\beta = \{1, 3, 4, 7\}$.

Hence, from Fig. 2, the number of UEs is proportional to the pilot symbols. Reducing the SINR required the selection of the optimum number of antennas because an increase in the number of antennas directly increased the SINR. The linear precoding R-ZF scheme, which could generate the identified user capacity and satisfy the SINR requirements, showed that the R-ZF was more efficient where it was able to mitigate pilot contamination in both intra- and inter-user interference. This depended on using the same users K in each cell and the same distance in km from the BS to the cells. Consequently, the R-ZF was better than ZF and MRT because it was able to suppress the SINR.

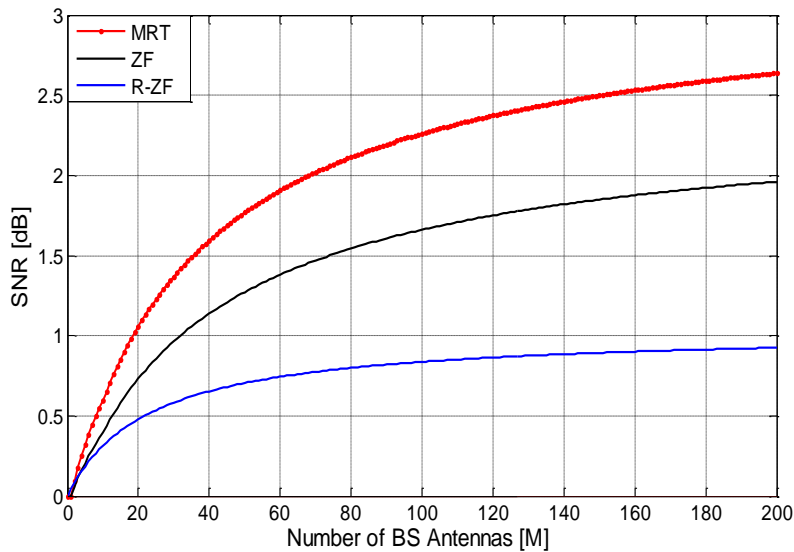


Fig. 2 SINR achieved when using many antennas M with different pilot symbols.

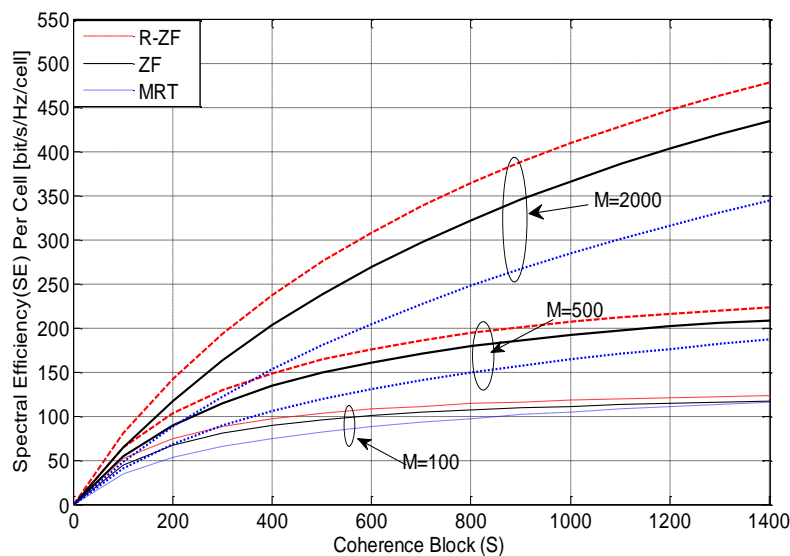


Fig. 3 The effects of the SE per cell with the coherence block length for an increasing number of antennas M .

In Fig. 3, it is noted that the coherence block length S is dependent on the number of UEs per cell. Consequently, the length of the coherence block affected the schedule of UEs per cell if $S = 600$. At a number of BS antenna $M = 100$, the ratio of M/K was relatively small because the cell contained more than 1000 randomly distributed users inside the cell. Therefore, we could not schedule more UEs as the number of antennas M at the BS was small. Moreover, the UEs increased slightly in number with S . However, with the increasing number of BS antennas $M = 2000$, we could schedule more of the number of UEs. This is the purpose of using the coherence block length S to schedule the number of UEs. This enhanced the SE with an increase in the number of antennas M and a large number of UEs. On the other hand, we can conclude that, with a scheduled increase, the number of UEs reduced the inter-cell between adjacent cells.

From Fig. 4, the relation between achievable SE and scheduled number of UEs K , is very important. From Fig. 4, it shows that linear precoding schemes such as MRT, ZF, and R-ZF chose the maximum number of UEs at larger and smaller values for different values of SE. Where, the increase number of users in every cell depends on the number of propagation channel $F_{j,e}^{\Omega}$. Consequently, a fixed number of UEs K provided the maximal SE depending on the number of antennas at the BS. Otherwise, from Fig. 4, when the number of antennas $M = 20$, we obtained the least value of SE. However, with an increase in the number of antennas $M = 500$, we obtained the maximum SE with the optimal number of UEs K . Consequently, R-ZF precoding scheme produces better values of SE than ZF and MRT. In addition, the number of antenna arrays at the BS had the same small value in both ZF and R-ZF, while, in MRT, it had different values at $M = 20$. On the other hand, with the increase in the number of antennas $M = 150$, every ZF and R-ZF was slightly separated. Based on Fig. 4, the SE started to increase when the number of K is small and the maximum SE can be achieved dependent on the optimal number of K . After this value, the SE starts to decrease with larger number of K .

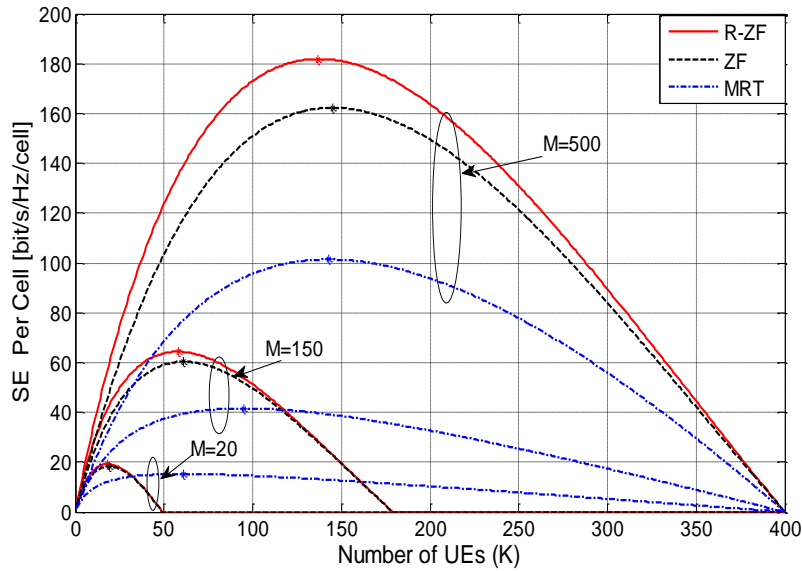


Fig. 4 Selected number of UEs with optimal SE.

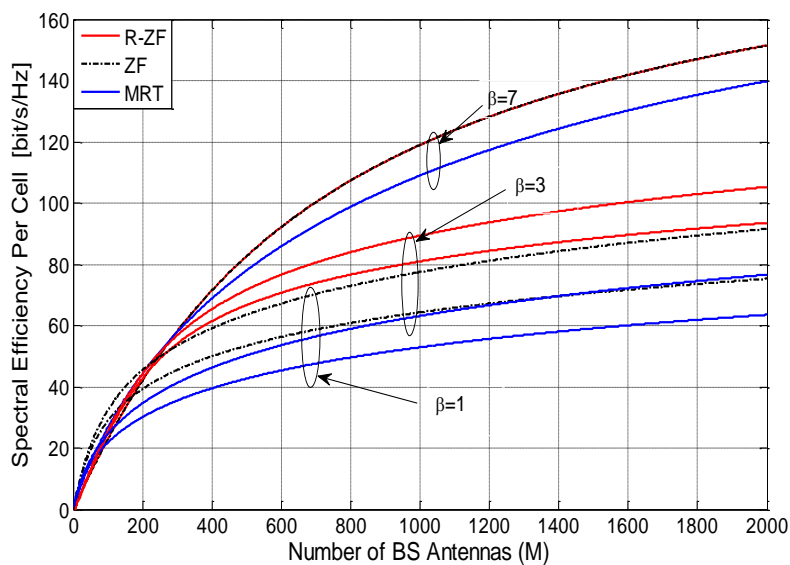


Fig. 5 Relation between the number of antennas and SE of using the pilot sequences.

From Fig. 5, to obtain the maximum SE with the rise in the number of antennas M , it was necessary to utilize a different pilot reuse sequence at the sending of many signals in downlinks between neighboring cells in the same cluster.

Consequently, it is noted from Fig. 5 that the R-ZF technique gave better values than ZF and MRT, using $\beta = \{1, 3, 4, 7\}$. Consequently, using different return pilot reuse sequences at $\beta = 7$, we obtained a maximum value of SE because it was able to avoid interference between adjacent cells, giving a better result than $\beta = 4$, $\beta = 3$, and $\beta = 1$. Otherwise, in order to employ different pilot reuses $\beta = 7$, the precoding scheme had to have the same value in both R-ZF and ZF. In comparison, it had different values for the use of linear scheme MRT because the two techniques were able to suppress intra-cell interference and interference between the neighboring cells because of its low sensitivity to SINR. At $\beta = 3$, the R-ZF gave a better value than the ZF and MRT.

But when comparing the SE at pilot reuse $\beta = 3$ with that at $\beta = 7$, when the number of recall reuse pilot within the channel, increased, the performance of SE was weak. So we conclude that, with the increase in the number of different pilot sequences, the transmitted signals in the downlinks of the channels could be improved using perfect CSI and intra-cell suppression in the same cell and interference between neighboring cells.

4. Conclusions

The massive MIMO system supported data rate improvements in the cell edges of 5G networks, where the technique facilitated coverage in the area and a high data rate at the edge of the cell. Avoiding the noise in the cell edge and guaranteeing the same performance in other cells require using large number of pilot reuse sequences. Moreover, it required a large β for higher channel estimation and the suppression of inter-cell-interference to improve SE. This involved the employment of different pilots, reusing them in different cells. The R-ZF technique gave better values than the ZF and MRT techniques at $\beta = \{1, 3, 4, 7\}$, where the employment of different pilot reuse at $\beta = 7$ resulted in better performance and gave the maximum value of SE. The use of $\beta = 7$ made it possible to avoid interference between adjacent cells and gave better results than the use of $\beta = 4$ and $\beta = 3$. This eliminated SINR through the use of R-ZF, ZF, and MRT. Finally, we conclude that the increase number of pilot reuse in downlink was able to provide better estimation quality and reduced the performance loss.

Acknowledgement

This work was supported by the Ministry of Higher Education Malaysia under the Fundamental Research Grant Scheme (FRGS) (V.1627).

References

- [1] Marzetta, T. L. (2010). Noncooperative cellular wireless with unlimited numbers of base station antennas. *IEEE Trans. Wireless Communication.*, 9(11), 3590–3600.
- [2] Baldemair, R. Dahlman, E. & Balachandran, K. (2013). Evolving wireless communications: Addressing the challenges and expectations of the future. *IEEE Veh. Technol. Mag.*, 8(1), 24–30.
- [3] Larsson, E.G., Tufvesson, F. Edfors, O. & Marzetta, T. L. (2014). Massive MIMO for next generation wireless systems. *IEEE Commun. Mag.*, 52(2), 186–195.
- [4] Lu, L., Li, G. Y. Swindlehurst, A. L. Ashikhmin, A. & Zhang, R. (2014). An overview of massive MIMO: Benefits and challenges. *IEEE J. Sel. Topics Signal Process.*, 8(5), 742–758.
- [5] Khormuji, M. N. (2016). Pilot-decontamination in massive MIMO systems via network pilot-data alignment. *IEEE International Conference on Communications Workshops (ICC)*, Kuala Lumpur, Malaysia, 93-97.
- [6] Björnson, E., Larsson, E.G. & Debbah, M. (2016). Massive MIMO for maximal spectral efficiency: How many users and pilots should be allocated?. *IEEE Transactions on Wireless Communications.*, 15(2), 1293-1308.
- [7] Jose, J. Ashikhmin, A. Marzetta, T. L. & Vishwanath S. (2011). Pilot contamination and precoding in multi-cell TDD systems. *IEEE Trans. Commun.*, 10(8), 2640–2651.
- [8] Li, X. Björnson, E. Larsson, E.G. Zhou, S. & Wang, J. (2017). Massive MIMO with multi-cell MMSE processing: exploiting all pilots for interference suppression. *EURASIP Journal on Wireless Communications and Networking*, 1, 2-15.
- [9] Stankovic, V. & Haardt, M. (2008). Generalized design of multiuser MIMO precoding matrices. *IEEE Trans. Wireless Commun.*, 7(3), 953 – 961.
- [10] Chae, C. B. & Heath, R. W. (2009). On the optimality of linear multiuser MIMO beamforming for a two-user two-input multiple-output broadcast system. *IEEE Signal Process. Letter*, 16(12), 117–120.
- [11] Salh, A. Audah, L. Shah, N. S. M. & Hamzah, S. A. (2019). Pilot Reuse Sequences in Downlink Multi-cells to Improve Data Rates in Massive MIMO System. *TELKOMNIKA Telecommunication Computing Electronics and Control*, 17(5), 101-108.
- [12] Zhu, X., Wang, Z. Dai, L. & Qian, C. (2015). Smart pilot assignment for massive MIMO. *IEEE Commun. Letter*, 19(9), 1644 –1647.

- [13] Yang, H. H. & Quek, T. Q. (2017). *Massive MIMO for Interference Suppression: Cell-Edge Aware Zero Forcing*. Springer International Publishing, 9 -34.
- [14] Jin, S. Wang, X. Li, Z. & Wong, K.K. (2014). Zero-forcing beamforming in massive MIMO systems with time-shifted pilots. *IEEE International Conference In Communications (ICC)*, Sydney, NSW, Australia, 4801-4806.
- [15] Xu, P. Wang, J. & Wang, J. (2013). Effect of pilot contamination on channel estimation in massive MIMO systems. *IEEE Int. Conf. Wireless Commun. and Signal Processing*, Hangzhou, China, 1–6.
- [16] Axel, M. Couillet, R. Bjornson, E. Wagner, S. & Debbah, M. (2015). Interference-aware R-ZF precoding for multicell downlink systems. *IEEE Trans. Signal Processing*, 63(15), 3959–3973.
- [17] Salh, A. Audah, L. Shah, N. S. M. & Hamzah, S. A. (2017). Reduction of pilot contamination in massive MIMO system. *IEEE Asia Pacific Microwave Conference (APMC)*, Kuala Lumpur, Malaysia, 885-888.